Antarctic Ice Sheet elevation impacts on water isotope records during the Last Interglacial

Sentia Goursaud[1], Max Holloway[2], Louise Sime[3], Eric Wolff[1], Paul Valdes[4], Eric J. Steig[5], Andrew Pauling[5]

[1]Department of Earth Sciences, University of Cambridge, UK
[2]Scottish Association for Marine Science, Oban, UK
[3]Ice Dynamics and Paleoclimate, British Antarctic Survey, Cambridge, UK
[4]School of Geographical Science, University of Bristol, Bristol, UK
[5]Department of Atmospheric Sciences, University of Washington, Seattle, US

Key Points:

- The relationship of δ^{18}O against elevation at 128 kyr is not uniform across Antarctica.
- The effect of the elevation can be isolated from that due to sea-ice change.
- Ice core results appear to unequivocally exclude the loss of the Wilkes Basin at around 128 ky.

Corresponding author: Sentia Goursaud, sg952@cam.ac.uk

Abstract

Changes of the topography of the Antarctic ice sheet (AIS) can complicate the interpretation of ice core water stable isotope measurements in terms of temperature. Here, we use a set of idealised AIS elevation change scenarios to investigate this for the warm Last Interglacial (LIG). We show that LIG δ^{18}O against elevation relationships are not uniform across Antarctica, and that the LIG response to elevation is lower than the preindustrial response. The effect of LIG elevation-induced sea ice changes on δ^{18}O is small, allowing us to isolate the effect of elevation change alone. Our results help to define the effect of AIS changes on the LIG δ^{18}O signals, and should be invaluable to those seeking to use AIS ice core measurements for these purposes. Especially, our simulations strengthen the conclusion that ice core measurements from the Talos Dome core exclude the loss of the Wilkes Basin at around 128 ky.

Plain Language Summary

The Last Interglacial period (LIG, 116,000 to 130,000 years ago) was globally $\sim$ 0.8 °C warmer than today at its peak, with substantially more warming at the poles. It is a valuable analogue for future global temperature rise, especially for understanding rates and sources of polar ice melt and subsequent global sea level rise. Records of water stable isotopes from Antarctic ice cores have been crucial for understanding past polar temperature during the LIG. However we currently lack a framework for estimating how changes in the ice sheet elevation, alongside sea-ice feedbacks, affect these water stable isotopes. To address this, we examine the effect of the Antarctic Ice Sheet (AIS) elevation on water stable isotopes, using an ensemble of climate simulations where we vary the AIS elevation. We observe that (i) water stable isotope values lower with increasing AIS elevation following linear relationships, (ii) the effect of sea-ice induced by AIS elevation is small so the effect of AIS elevation can be isolated. Finally, this study provides appropriate elevation-water stable isotope gradients for the reconstruction of the AIS topography using ice cores.

1 Introduction

The size and configuration of the Antarctic Ice Sheet (AIS) varies in response to mass balance (Scambos et al., 2017) and ice dynamics. Variations in the rate of accumulation are important across the continent (Ritz et al., 2001; Steig et al., 2013). Current West Antarctic Ice Sheet (WAIS) changes are driven by increasing melt, calving rates, and associated ice flow changes. These processes are sensitive to ocean temperature, alongside ocean and atmospheric circulation changes (Pollard & DeConto, 2009; DeConto & Pollard, 2016; Scambos et al., 2017; Adusumilli et al., 2020).

Geological data indicate that the WAIS expanded during the Last Glacial Maximum (LGM, approximately 21 kyears BP (ka)) (Conway et al., 1999; Bentley et al., 2014), and likely reduced during warmer interglacials (Scherer et al., 1998; McKay et al., 2012; Kopp et al., 2009, 2013; Dutton et al., 2015; Steig et al., 2015; DeConto & Pollard, 2016). It is less clear if the East AIS also reduced or expanded during interglacials (Wilson et al., 2018; Sutter et al., 2020). Last Interglacial (LIG) changes in insolation are also known to directly impact polar sea ice extent (Guarino et al., 2020; Kageyama et al., 2020).

It has been difficult to explain the LIG peak in δ^{18}O at 128 ky in Antarctic ice core data (Sime et al., 2009). Holloway et al. (2016) provided a potential explanation for the observed signal, but we still lack understanding of how elevation, insolation and sea ice jointly affect the water isotope signal. Since insolation and sea ice, in addition to AIS change, affect the isotopic signal in ice cores (Holloway et al., 2016, 2017; Malmierca-Vallet et al., 2018), it is necessary to understand how temperature, atmospheric circulation, spatially variable lapse rates, and sea ice feedbacks can all affect the recorded ac-

cumulation and isotopic signals when attempting to use these data to help us to deduce past AIS changes.

Werner et al. (2018); Sutter et al. (2020) explored the use of δ^{18}O (and temperature) versus elevation relationships to help to evaluate possible AIS reconstructions. Werner et al. (2018) focused on the LGM using the isotope-enabled atmospheric general circulation model ECHAM5-wiso to produce a set of LGM simulations with different AIS reconstructions used in the framework of the Paleoclimate Modelling Intercomparison Project (Otto-Bliesner et al., 2017). A model-data (ice core) δ^{18}O comparison allowed insight into the most likely LGM AIS configuration. More recently, Sutter et al. (2020) derived the most probable Wilkes configuration for the LIG by comparing δ^{18}O anomalies from the Talos Dome ice core with a suite of ice sheet model simulations using the Parallel Ice Sheet Model (Golledge et al., 2015). Sutter et al. (2016) inferred the LIG δ^{18}O signal for each of their model configurations using the present-day SAT versus elevation relationship from Frezzotti et al. (2007) to obtain temperature, and then to apply the SAT versus temperature derived from Werner et al. (2018). More generally, obtaining quantified information on LIG AIS loss from ice core measurements is still needed for the LIG community (Sime et al., 2019). The LIG AIS loss scenario is directly relevant to calculating future AIS loss probabilities (e.g. DeConto & Pollard, 2016; Edwards et al., 2019).

Here we investigate the stable water isotope (δ^{18}O) response to changes in AIS elevation at 128 ky, using an ensemble of isotope-enabled climate model experiments from the HadCM3 model. We describe the patterns of surface air temperature (SAT), precipitation and δ^{18}O in response to elevation changes, and compare isotope-elevation relationships at the continental scale as well as at the location of ice cores spanning the LIG. Finally, we briefly discuss how our results might be used to help to interpret LIG isotope signatures.

2 Materials and Methods

The isotopic response to idealised changes in AIS elevation is simulated using the isotope-enabled coupled ocean–atmosphere–sea-ice General Circulation Model, HadCM3 (Tindall et al., 2009). Fractional isotopic content is expressed for oxygen-18 using standard δ^{18}O notation (Supporting Information, Text S1). Two control simulations were used: a preindustrial (PI) simulation, and a 128 ka simulation centred on the LIG Antarctic isotope maximum using a modern day AIS configuration (Holloway et al., 2016). Then a suite of eight idealised AIS elevation change simulations were performed also including 128 ka orbital and greenhouse-gas forcing. Each elevation change experiment includes a simple scaling of the AIS to isolate the impact of ice sheet elevation on temperature, precipitation and δ^{18}O. The change in elevation across the AIS is scaled relative to the prescribed change at the EPICA Dome C (EDC) ice core site using a scaling coefficient β, where:

$$\beta = \frac{Z_{EDC}}{(Z_{EDC} + \Delta z)}, \tag{1}$$

and Z_{EDC} is the EDC ice core site elevation in the modern day AIS configuration, Δz is the prescribed elevation change at EDC, which extends to $\pm$ 1000 m. Elevations across the Antarctic continent are then increased or decreased proportional to β;

$$Z_A^{'} = Z_A/\beta \tag{2}$$

where Z_A is the two-dimensional array of modern AIS elevations and $Z_A^{'}$ is a new array of altered AIS elevations. Since this approach maintains the modern shape of the AIS, it reduces the influence of changing ice sheet configuration on circulation and climate and helps in isolating the effect of elevation changes alone. Experiments are performed with Δz equal to (+/-) 100, 200, 500 and 1000 m (Supporting Information, Table S1). Each of the above elevation change scenarios is integrated for a total of 500-years to ensure that surface and mid-depth climate fields are sufficiently spun-up with the imposed

elevation changes. The last 50 years of each simulation are analysed. We also include a simulation with the WAIS reduced to a uniform elevation of 200 m and remains ice covered, as published in Holloway et al. (2016), and following the approach of Holden et al. (2010).

LIG maximum values of +2-4 ‰ above PI in δ^{18}O are recorded in East Antarctic ice cores. We consider our elevation scenarios in the context of these LIG δ^{18}O published ice core records from East Antarctica (Masson-Delmotte et al., 2011): Vostok (Petit et al., 1999), Dome Fuji (DF, Kawamura et al., 2007), EPICA Dome C (EDC, Jouzel et al., 2007), EPICA Dronning Maud Land (EDML, EPICA Community Members, 2006) Talos Dome Ice Core (TALDICE, Stenni et al., 2011), and Taylor Dome (Steig et al., 2000), as well as unpublished or planned LIG δ^{18}O ice core records from West Antarctica: West Antarctica Ice Sheet Divide, Hercules Dome and Skytrain.

For all our statistical analyses, averages are given with their associated standard deviation (average ± standard deviation). Linear relationships are considered significant when the p-value is lower than 0.05 (Supporting Information, Text S2).

3 Results

3.1 Changes in Antarctic surface air temperature and precipitation

The LIG forcing, with no AIS elevation change, induces a mean annual Antarctic warming of 0.9 ± 0.6 °C compared to PI (Supporting information, Table S2); and precipitation increases of 0.6 ± 1.3 mm/month. Changes are larger in the coastal regions and show wider regional differences: for example, precipitation increases on the coast of the Bellingshausen Sea but decreases on the coast of the Amundsen Sea (c.f. Otto-Bliesner et al., 2020).

Increases in the elevation of AIS act to decrease surface air temperatures (SAT) (Mechoso, 1980, 1981; Parish et al., 1994; Singh et al., 2016). The mean Antarctic SAT change is +4.7 ± 4.6 °C higher for the DC-1km experiment; and −4.4 ± 4.2 °C for the DC+1km experiment, compared to the LIG control simulation (Figure 1).

Changes in precipitation with the elevation tend to follow SAT changes, i.e. it decreases as the elevation of AIS is increased. Mean Antarctic precipitation anomalies compared to the LIG control simulation are 3.0 ± 4.7 mm/month for the DC-1km experiment, and -2.4 ± 4.2 mm/month for the DC+1km experiment. The largest changes in precipitation occur along coasts facing the Indian Ocean, the Weddell Sea and along the Ronne Ice Shelf, where the orographic slopes are the steepest (Supporting information, Figure S1; Krinner & Genthon, 1999). Deviations from the SAT-precipitation relationships are also the largest in coastal areas (Figure 1). In particular the Eastern part of the Peninsula and the WAIS coast display opposite elevation-precipitation relationships compared to the rest of the AIS. This may be due to changes in the localised Peninsula foehn-related drying and/or heat fluxes associated with a more stationary Amundsen Sea low when AIS topography is higher (Krinner & Genthon, 1999). These factors are liable to cause complications when interpreting accumulation change data from coastal and Peninsula ice cores during AIS changes (e.g. Medley & Thomas, 2019).

3.2 Antarctic ice core δ^{18}O anomalies

Mean Antarctic δ^{18}O increases during the LIG by 0.6 ± 0.8 ‰ compared to PI. At the continental scale, when changing the entire AIS elevation, δ^{18}O changes closely follow both SAT and elevation (Figures 1 and 2). This result is consistent with Holloway et al. (2016) and Steig et al. (2015), who report strong positive anomalies over the WAIS when WAIS elevations are reduced to 200 m ("Flat WAIS" experiment hereafter). Our results indicate that δ^{18}O anomalies against PI are stronger when the elevation is de-

creased than when the elevation is increased, a feature also observed for SAT. For the DC-1km simulation, mean Antarctic δ^{18}O changes is +6.5 ± 2.9 ‰, compared to the PI simulation; and −2.3 ± 2.4 ‰ for the DC+1km simulation. However, there are heterogenous patterns in δ^{18}O anomalies - mainly in East Antarctica - in response to our idealised and linear elevation changes.

Figure 2 (and Supporting information Table S3) includes the δ^{18}O changes at existing and planned ice core drilling sites. Since these are idealised topographies, and there are other influences on δ^{18}O, it is not surprising that none of the simulated elevation changes provide a match to the PI to LIG δ^{18}O differences observed in ice cores (Supporting information, Table S4). The results of Holloway et al. (2016) show that a reduction in winter sea ice area of 65 ± 7 % provide a closer match to the ice core data than any of the idealised AIS elevation change simulations presented here; it is thus of interest to understand how changes in ice sheet elevation and sea ice interact, which will be discussed below.

3.3 The impact of AIS-sea ice feedbacks on δ^{18}O, temperature and precipitation

Antarctic sea ice extent increases by 7.6 % for the DC-1km experiment and decreases by 10.8 % for the DC+1 km experiment (Figure 1). This confirms the AIS feedback on sea ice identified by Singh et al. (2016) (for the case of a 90 % flattening of AIS compared to PI). Changes in surface wind stress affect the westerly momentum transfer to the ocean (Schmittner et al., 2011), modulating Northward Ekman transport and the associated Ekman drift of sea ice (Singh et al., 2016). In our simulations, a decrease in AIS elevation results in a noticeable reduction of the easterlies around 72 °S and westerlies around 52 °S (of approximately 8% and 5%, respectively, for DC-1 km), but with little shift in the maximum latitudes of wind speed (Supporting information, Figure S2). These changes are likely driven via katabatic-easterlies-westerlies interactions (Sime et al., 2013) and are important to explain the simulated sea ice changes: under DC-1km a smaller volume of sea ice is pushed north, towards warmer waters.

However, it is noteworthy that the sea ice changes can be modified if WAIS and East Antarctic Ice Sheet (EAIS) are adjusted independently; Steig et al. (2015) found a decrease in sea ice extent with a decrease in WAIS elevation. Thus, the sign of sea ice change depends on the details of the topographic change.

Even for our simple linearly scaled-AIS scenarios, sea ice changes are spatially non-uniform around Antarctica. Sea ice extent changes are particularly variable with respect to AIS elevation in the Bellingshausen sector: a 50 % increase occurs for the DC-1km experiment (Supporting information, Table S4 and Figure S3). This is likely also related to differing wind forcing, and thus sea ice export, associated with a more stationary and stronger Amundsen Sea low when AIS topography is lower (Krinner & Genthon, 1999; Steig et al., 2015). The Weddell sector shows particularly small changes (± 5 %). Variability in other sectors remains within a ± 15 % range. The Bellingshausen and Weddell sectors also stand out in that they present non-linear AIS-sea ice relationships. Considering the other sectors separately, the mean rate of sea ice area change is -1 % per 100 m of elevation change at Dome C (with a mean correlation coefficient of 0.93 and a p-value < 0.05).

In terms of their control on temperature, precipitation and δ^{18}O, these sea ice changes are small compared with the changes in sea ice explored in Holloway et al. (2016). Removing the AIS-sea ice feedbacks on δ^{18}O using a linear relationship (Supporting information, Figure S4) has a very small effect on precipitation (-3.0 ± 1.7 % and 4.4 ± 2.4 % changes compared to the LIG control simulation for the DC+1km and DC-1km simulations respectively), SAT (0.4 ± 0.5 % and -0.5 ± 0.7 % changes compared to the LIG control simulation for the DC+1km and DC-1km simulations respectively) and δ^{18}O anoma-

lies (0.9 ± 0.4 % and -1.4 ± 0.6 % changes compared to the LIG control simulation for the DC+1km and DC-1km simulations respectively).

The small size of the these indirect AIS-sea ice mediated impacts on temperature, precipitation, and δ^{18}O lends confidence to the strategy of treating AIS and sea ice change impacts on δ^{18}O as effectively independent of each other (Holloway et al., 2016; Chadwick et al., 2020; Holloway et al., 2017). In the following, we thus consider we can quantify the δ^{18}O versus elevation relationship independently from other effects.

3.4 Linear SAT- and δ^{18}O-elevation relationships

Werner et al. (2018); Sutter et al. (2020) explored the use of δ^{18}O (and SAT) versus elevation relationships to help to evaluate possible AIS reconstructions for the LGM and LIG respectively. In each case they used a linear relationship between climate variables and elevation to ascertain past AIS changes. Here we can use our simulations to assess whether the SAT and δ^{18}O versus elevation relationships used in these studies are supported by our suite of LIG simulations. To do this, we calculate slopes for these relationships, using all simulations on a grid-point-by-grid-point basis (Figure 3 and Figure 4, and Supporting information, Text S2).

The Ross Sea, Amundsen Sea and the coastal regions ($\leq$ 1000 m a.s.l) show no significant linear relationships, likely because the inter-simulation noise in these quantities is larger than the signal, due to the small elevation changes prescribed in these regions. Outside these regions, where elevation changes are larger, slopes increase from the coast to the plateau. Mean slopes for ΔSAT versus elevation are -0.34 ± 0.24 °C/100 m for regions currently between 1000 and 2000 m a.s.l. This rises considerably to -0.92 ± 0.11 °C/100 m for regions above 3000 m a.s.l (Supporting information, Table S5). In both case these differ from the present-day spatial ΔSAT versus elevation documented by Frezzotti et al. (2007, -0.8 °C/100 m) and Masson-Delmotte et al. (2008, -1.1 °C/100 m) (and subsequently used by other authors to calculate past elevation changes). Correlation coefficients for ΔSAT - elevation are higher than 0.9 for all the grid points with significant relationships.

Changes in precipitation (ΔP) and $\Delta\delta^{18}$O versus elevation have lower correlation coefficients compared to SAT-elevation relationships, especially on the plateau. Unlike for the SAT-elevation relationships, δ^{18}O-elevation slopes are higher in coastal regions compared to the plateau, likely due to source-distance effects on ΔP and, subsequently, $\Delta\delta^{18}$O (Figure 3). This feature is also notable at the ice core locations (Figure 4). The variability of $\Delta\delta^{18}$O versus elevation slopes is also spatially larger than for ΔSAT (and ΔP); they vary from -1.28 ± 1.38 ‰/100 m for regions between 1000 and 2000 m a.s.l to -0.53 ± 0.22 ‰/100 m for regions above 3000 m a.s.l. This high variability is also reflected in the $\Delta\delta^{18}$O versus elevation calculated at ice core locations (Supporting information, Table S6), with the largest slope at the coastal Skytrain location (-3.52 ‰/100) and smallest slopes on the EAIS plateau e.g. -0.48 ‰/100 m at EDML.

Comparing our simulated relationships to those used by Sutter et al. (2020) to interpret the TALDICE δ^{18}O ice core measurements, our simulations would suggest that the relationship used in Sutter et al. (2020) would underestimate the sensitivity of $\Delta\delta^{18}$O to elevation change by 43 % in this region (Supporting information, Text S3): they use a SAT versus elevation slope of -0.8 °C/100 m (which seems to be an overestimate, see Table S6) multiplied by a δ^{18}O versus temperature slope of 0.66 ‰/°C, to obtain a δ^{18}O-elevation relationship of -0.53 ‰/100 m. a δ^{18}O-elevation relationship of 0.53 ‰/100 m. These relationships were inferred from present-day values, whereas it might have changed with time. Using our simulations, we thus look at the $\Delta\delta^{18}$O versus elevation relationship (LIG temporal relationship) and show that this relationship at this site is -0.93 ‰/100 m. For the elevation change they simulate in the case of Wilkes Basin ice collapse, using our LIG temporal relationship, this would lead to an inferred TALDICE δ^{18}O increase

from 11 to 19 ‰, i.e., 73 to 83 % higher than suggested. This implied underestimation of the inferred δ^{18}O from the grounding retreat, reinforces the conclusions of Sutter et al. (2020), emphasizing that TALDICE is an highly sensitive site for indicating EAIS LIG changes, and exclude the Wilkes Basin loss of ice scenarios, since the TALDICE LIG-PI δ^{18}O measured change is only 2 ‰ (Masson-Delmotte et al., 2008).

One of the reasons for the mismatch between our and the Sutter et al. (2020) calculations is their use of a relationship between δ^{18}O-temperature not specific to LIG, in the use of calculating past AIS change. Indeed, as for Werner et al. (2018), we find different relationships for different times. If we use all grid-points above 100 m a.s.l., a continent-wide average of the slope yields -0.83 ± 0.71 ‰/100m (r = -0.9). This LIG-PI $\Delta\delta^{18}$O-elevation slope is similar to, but slightly higher than the LGM-PI slope obtained by Werner et al. (2018) (slope of -0.71 ± 0.3 ‰/100m). Similarly to Werner et al. (2018), we thus obtain a continent-wide temporal $\Delta\delta^{18}$O-elevation slope, which is 30 % lower than the observational present-day spatial δ^{18}O-elevation slope (slope of -1.0 ‰/100 m, r=-0.9, Masson-Delmotte et al., 2008) and the HadCM3 simulated one (slope of -1.07 ± 0.02 ‰/100 m, r=-0.89). This, alongside the above, confirms that ~~the use of~~ a present-day spatial elevation gradient as a surrogate for temporal changes for LIG-PI changes must be done with a great deal of care, as it may be incorrect for a variety of locations, AIS changes, and changes through time. Finally we note that, as suggested by Sime et al. (2009); Noone (2009), Figure 4 clearly shows that for a variety of locations, $\Delta\delta^{18}$O does not vary in a linear way, so the use of any single gradient, even for a given ice core site, may vary with time and elevation.

4 Conclusions

Overall, we see that elevation-induced changes in δ^{18}O follow those in SAT. Larger changes in SAT with elevation occur in coastal regions compared to the plateau. Whilst both δ^{18}O and precipitation tend to follow SAT changes when site elevation changes, differences do occur in East Antarctic coastal areas where the orographic slope is high. Compared to the eastern part, the Peninsula and WAIS coastal regions display opposite trends, i.e. increasing (decreasing) precipitation with increasing (decreasing) AIS elevation. This suggests the need to (i) employ caution, (ii) model δ^{18}O and (iii) drill other ice core species according to accurate WAIS change scenarios to understand how WAIS change will imprint on WAIS ice cores. We note that Antarctic sea ice extent has a relatively modest response to our elevation change experiments. This leads to a small feedback of elevation on climate parameters through sea ice, and tends to support the approach that we can look at the controls of sea ice and AIS change on ice core measurements independently (Holloway et al., 2016, 2017).

We find a continental-wide average of the $\Delta\delta^{18}$O versus elevation relationship of -0.83 ± 0.71 ‰/100 m (r = -0.9 ± 0.29), thus 20 % lower than the PI spatial slope, confirming that the spatial PI δ^{18}O versus elevation relationship cannot be a surrogate for temporal relationships (Werner et al., 2018). We find that relationships vary significantly between different ice core locations, ranging from -3.52 ‰/100 m at Skytrain to -0.48 ‰/100 m at EDML.

Confidently dated ice core measurements covering the LIG are currently only available from East Antarctic ice core sites. Given the widespread expectation of major changes in WAIS elevation during the LIG, there is a need for new well dated ice cores covering the LIG from sites outside the EAIS, alongside further δ^{18}O modelling. New ice cores drilled on the WAIS, particularly at Skytrain or Hercules Dome will provide important insights for future AIS LIG reconstructions. The results above enable ice core δ^{18}O measurements to be interpreted from an elevation point-of-view with more certainty.

Finally, we note that this study is limited by the model resolution of HadCM3 and our particular simulation set-up: prescribing small absolute changes in elevation in coastal regions. The Skytrain site would thus benefit from high-resolution modelling, ideally using a regional isotope-enabled climate model.

5 Data

The orography, surface air temperature, precipitation and water stable isotope responses to idealised changes in AIS elevation simulated by the isotope-enabled coupled ocean–atmosphere–sea-ice General Circulation Model HadCM3, are available on the data system managed by the UK Polar Data Centre (Goursaud et al., 2020) under the Open Government License (http://www.nationalarchives.gov.uk/doc/open-government-licence/version/3/).

Acknowledgments

S.G., E.W.W, and L.C.S were funding through the European Research Council under the Horizon 2020 research and innovation programme (grant agreement No 742224, WACSWAIN). E.W.W. is also supported by a Royal Society Professorship. L.C.S. and M.H. acknowledge support through NE/P013279/1, NE/P009271/1, and EU-TiPES. The project has received funding from the European Unions Horizon 2020 research and innovation programme under grant agreement No 820970. This material reflects only the authors views and the Commission is not liable for any use that may be made of the information contained therein.

References

Adusumilli, S., Fricker, H. A., Medley, B., Padman, L., & Siegfried, M. R. (2020). Interannual variations in meltwater input to the southern ocean from antarctic ice shelves. *Nature Geoscience*, 1–5.

Bazin, L., Landais, A., Lemieux-Dudon, B., Toyé Mahamadou Kele, H., Veres, D., Parrenin, F., ... Wolff, E. (2013). An optimized multi-proxy, multi-site antarctic ice and gas orbital chronology (aicc2012): 120ndash;800 ka. *Climate of the Past*, *9*(4), 1715–1731. Retrieved from `https://cp.copernicus.org/articles/9/1715/2013/` doi: 10.5194/cp-9-1715-2013

Bentley, M. J., Cofaigh, C. ., Anderson, J. B., Conway, H., Davies, B., Graham, A. G., ... Zwartz, D. (2014). A community-based geological reconstruction of antarctic ice sheet deglaciation since the last glacial maximum. *Quaternary Science Reviews*, *100*, 1 - 9. Retrieved from `http://www.sciencedirect.com/science/article/pii/S0277379114002546` (Reconstruction of Antarctic Ice Sheet Deglaciation (RAISED)) doi: https://doi.org/10.1016/j.quascirev.2014.06.025

Chadwick, M., Allen, C., Sime, L., & Hillenbrand, C.-D. (2020). Analysing the timing of peak warming and minimum winter sea-ice extent in the southern ocean during mis 5e. *Quaternary Science Reviews*, *229*, 106134.

Conway, H., Hall, B. L., Denton, G. H., Gades, A. M., & Waddington, E. D. (1999). Past and future grounding-line retreat of the west antarctic ice sheet. *Science*, *286*(5438), 280–283. Retrieved from `http://science.sciencemag.org/content/286/5438/280` doi: 10.1126/science.286.5438.280

DeConto, R. M., & Pollard, D. (2016). Contribution of antarctica to past and future sea-level rise. *Nature*, *531*(7596), 591–597.

Dutton, A., Carlson, A. E., Long, A. J., Milne, G. A., Clark, P. U., DeConto, R., ... Raymo, M. E. (2015). Sea-level rise due to polar ice-sheet mass loss during past warm periods. *Science*, *349*(6244). Retrieved from `http://science.sciencemag.org/content/349/6244/aaa4019` doi: 10.1126/science.aaa4019

Edwards, T. L., Brandon, M. A., Durand, G., Edwards, N. R., Golledge, N. R., Holden, P. B., ... Wernecke, A. (2019). Revisiting antarctic ice loss due to marine ice-cliff instability. *Nature*, *566*(7742), 58–64.

EPICA Community Members. (2006). One-to-one coupling of glacial climate variability in Greenland and Antarctica. *Nature*, *444*(7116), 195–198. Retrieved from `http://www.nature.com/doifinder/10.1038/nature05301` doi: 10.1038/nature05301

Frezzotti, M., Urbini, S., Proposito, M., Scarchilli, C., & Gandolfi, S. (2007). Spatial and temporal variability of surface mass balance near talos dome, east antarctica. *Journal of Geophysical Research: Earth Surface*, *112*(F2).

Golledge, N. R., Kowalewski, D. E., Naish, T. R., Levy, R. H., Fogwill, C. J., & Gasson, E. G. W. (2015). The multi-millennial antarctic commitment to future sea-level rise. *Nature*, *526*(7573), 421–425. doi: 10.1038/nature15706

Goursaud, S., Holloway, M., Sime, L., Wolff, E., Valdes, P., Steig, E., & Pauling, A. (2020). Global monthly outputs of orography, surface air temperature and water stable isotopes for the last interglacial for idealised antarctic ice sheet simulations run by the isotope-enabled hadcm3. doi: https://doi.org/10.5285/09330d14-7f2d-4c12-ad00-08a9cd1fb214

Guarino, M.-V., Sime, L. C., Schröeder, D., Malmierca-Vallet, I., Rosenblum, E., Ringer, M., ... others (2020). Sea-ice-free arctic during the last interglacial supports fast future loss. *Nature Climate Change*, 1–5.

Holden, P., Edwards, N., Wolff, E. W., Lang, N. J., Singarayer, J., Valdes, P., & Stocker, T. (2010). Interhemispheric coupling, the west antarctic ice sheet and warm antarctic interglacials. *Climate of the Past*, *6*(4), 431–443.

Holloway, M. D., Sime, L. C., Allen, C. S., Hillenbrand, C. D., Bunch, P., Wolff, E., & Valdes, P. J. (2017). The Spatial Structure of the 128 ka Antarctic Sea Ice Minimum. *Geophysical Research Letters*, *44*. doi: 10.1002/2017GL074594

Holloway, M. D., Sime, L. C., Singarayer, J. S., Tindall, J. C., Bunch, P., & Valdes, P. J. (2016, aug). Antarctic last interglacial isotope peak in response to sea ice retreat not ice-sheet collapse. *Nature Communications*, *7*, 12293. Retrieved from `http://dx.doi.org/10.1038/ncomms12293http://10.0.4.14/ncomms12293http://www.nature.com/articles/ncomms12293{\#}supplementary-information`

Jouzel, J., Masson-Delmotte, V., Cattani, O., Dreyfus, G., Falourd, S., Hoffmann, G., ... Wolff, E. W. (2007, aug). Orbital and millennial Antarctic climate variability over the past 800,000 years. *Science*, *317*(5839), 793–796. Retrieved from `http://www.ncbi.nlm.nih.gov/pubmed/17615306` doi: 10.1126/science.1141038

Kageyama, M., Sime, L. C., Sicard, M., Guarino, M. V., de Vernal, A., Schroeder, D., ... others (2020). A multi-model cmip6 study of arctic sea ice at 127ka: Sea ice data compilation and model differences. *Climate of the Past Discussions*.

Kawamura, K., Parrenin, F., Lisiecki, L., Uemura, R., Vimeux, F., Severinghaus, J. P., ... Watanabe, O. (2007). Northern Hemisphere forcing of climatic cycles in Antarctica over the past 360,000 years. *Nature*, *448*(7156), 912–916. doi: 10.1038/nature06015

Kopp, R. E., Simons, F. J., Mitrovica, J. X., Maloof, A. C., & Oppenheimer, M. (2009). Probabilistic assessment of sea level during the last interglacial stage. *Nature*, *462*, 863–868. doi: 10.1038/nature08686

Kopp, R. E., Simons, F. J., Mitrovica, J. X., Maloof, A. C., & Oppenheimer, M. (2013). A probabilistic assessment of sea level variations within the last interglacial stage. *Geophysical Journal International*. doi: 10.1093/gji/ggt029

Krinner, G., & Genthon, C. (1999). Altitude dependence of the ice sheet surface climate. *Geophysical research letters*, *26*(15), 2227–2230.

Malmierca-Vallet, I., Sime, L. C., Tindall, J. C., Capron, E., Valdes, P. J., Vinther, B. M., & Holloway, M. D. (2018). Simulating the last interglacial greenland stable water isotope peak: The role of arctic sea ice changes. *Quaternary Science Reviews*, *198*, 1–14.

Masson-Delmotte, V., Buiron, D., Ekaykin, a., Frezzotti, M., Gallée, H., Jouzel, J., ... Vimeux, F. (2011, apr). A comparison of the present and last interglacial periods in six Antarctic ice cores. *Climate of the Past*, *7*(2), 397–423. Retrieved from `http://www.clim-past.net/7/397/2011/` doi: 10.5194/cp-7-397-2011

Masson-Delmotte, V., Hou, S., Ekaykin, A., Jouzel, J., Aristarain, A., Bernardo, R. T., ... White, J. W. C. (2008, jul). A Review of Antarctic Surface Snow Isotopic Composition: Observations, Atmospheric Circulation, and Isotopic Modeling. *Journal of Climate*, *21*, 3359–3387. Retrieved from `http://journals.ametsoc.org/doi/abs/10.1175/2007JCLI2139.1` doi: 10.1175/2007JCLI2139.1

McKay, R., Naish, T., Powell, R., Barrett, P., Scherer, R., Talarico, F., ... Williams, T. (2012). Pleistocene variability of antarctic ice sheet extent in the ross embayment. *Quaternary Science Reviews*, *34*, 93–112. Retrieved from `http://www.sciencedirect.com/science/article/pii/S0277379111004057` doi: https://doi.org/10.1016/j.quascirev.2011.12.012

Mechoso, C. R. (1980). The atmospheric circulation around antarctica: Linear stability and finite-amplitude interactions with migrating cyclones. *Journal of the Atmospheric Sciences*, *37*(10), 2209–2233.

Mechoso, C. R. (1981). Topographic influences on the general circulation of the southern hemisphere: A numerical experiment. *Monthly Weather Review*, *109*(10), 2131–2139.

Medley, B., & Thomas, E. (2019). Increased snowfall over the antarctic ice sheet mitigated twentieth-century sea-level rise. *Nature Climate Change*, *9*(1), 34–39.

Noone, D. (2009). Kink in the thermometer. *Nature*, *462*(7271), 295–296.

Otto-Bliesner, B., Braconnot, P., Harrison, S., Lunt, D., Abe-Ouchi, A., Albani, S., ... others (2017). The pmip4 contribution to cmip6–part 2: Two interglacials, scientific objective and experimental design for holocene and last interglacial simulations.

Otto-Bliesner, B., Brady, E., Zhao, A., Brierley, C., Axford, Y., Capron, E., ... others (2020). Large-scale features of last interglacial climate: Results from evaluating the lig127k simulations for cmip6-pmip4. *Climate of the Past Discussions*.

Parish, T. R., Bromwich, D. H., & Tzeng, R.-Y. (1994). On the role of the antarctic continent in forcing large-scale circulations in the high southern latitudes. *Journal of the atmospheric sciences*, *51*(24), 3566–3579.

Petit, J. R., Raynaud, D., Basile, I., Chappellaz, J., Davisk, M., Ritz, C., ... Saltzmank, E. (1999). Climate and atmospheric history of the past 420,000 years from the Vostok ice core, Antarctica. *Nature*, *399*, 429–436.

Pollard, D., & DeConto, R. M. (2009, mar). Modelling West Antarctic ice sheet growth and collapse through the past five million years. *Nature*, *458*(7236), 329–32. Retrieved from `http://www.ncbi.nlm.nih.gov/pubmed/19295608` doi: 10.1038/nature07809

Ritz, C., Rommelaere, V., & Dumas, C. (2001). Modeling the evolution of Antarctic ice sheet over the last 420,000 years' Implications for altitude changes in the Vostok region. *JOURNAL OF GEOPHYSICAL RESEARCH*, *106*(D23), 943–974. doi: 10.1029/2001JD900232

Scambos, T., Bell, R., Alley, R., Anandakrishnan, S., Bromwich, D., Brunt, K., ... Yager, P. (2017). How much, how fast?: A science review and outlook for research on the instability of antarctica's thwaites glacier in the

21st century. *Global and Planetary Change*, *153*, 16–34. Retrieved from http://www.sciencedirect.com/science/article/pii/S092181811630491X doi: 10.1016/j.gloplacha.2017.04.008

Scherer, R. P., Aldahan, A., Tulaczyk, S., Possnert, G., Engelhardt, H., & Kamb, B. (1998). Pleistocene Collapse of the West Antarctic Ice Sheet. *Science*, *281*(5373), 82–85. Retrieved from http://dx.doi.org/10.1126/science.281.5373.82 doi: 10.1126/science.281.5373.82

Schmittner, A., Silva, T. A., Fraedrich, K., Kirk, E., & Lunkeit, F. (2011). Effects of mountains and ice sheets on global ocean circulation. *Journal of Climate*, *24*(11), 2814–2829.

Sime, L. C., Carlson, A., & Holloway, M. (2019). On recovering last interglacial changes in the antarctic ice sheet. *Past Global Changes Magazine*, *27*(1), 14–15.

Sime, L. C., Kohfeld, K. E., Le Quéré, C., Wolff, E. W., de Boer, A. M., Graham, R. M., & Bopp, L. (2013). Southern hemisphere westerly wind changes during the last glacial maximum: model-data comparison. *Quaternary Science Reviews*, *64*, 104–120.

Sime, L. C., Wolff, E. W., Oliver, K. I. C., & Tindall, J. C. (2009, nov). Evidence for warmer interglacials in East Antarctic ice cores. *Nature*, *462*, 342–345. Retrieved from http://www.ncbi.nlm.nih.gov/pubmed/19924212 doi: 10.1038/nature08564

Singh, H. K., Bitz, C. M., & Frierson, D. M. (2016). The global climate response to lowering surface orography of antarctica and the importance of atmosphere–ocean coupling. *Journal of Climate*, *29*(11), 4137–4153.

Steig, E. J., Ding, Q., White, J. W., Küttel, M., Rupper, S. B., Neumann, T. A., ... others (2013). Recent climate and ice-sheet changes in west antarctica compared with the past 2,000 years. *Nature Geoscience*, *6*(5), 372–375.

Steig, E. J., Huybers, K., Singh, H. A., Steiger, N. J., Ding, Q., Frierson, D. M., ... White, J. W. (2015). Influence of west antarctic ice sheet collapse on antarctic surface climate. *Geophysical Research Letters*, *42*(12), 4862–4868.

Steig, E. J., Morse, D. L., Waddington, E. D., Stuiver, M., Grootes, P. M., Mayewski, P. A., ... Whitlow, S. I. (2000). Wisconsinan and holocene climate history from an ice core at taylor dome, western ross embayment, antarctica. *Geografiska Annaler: Series A, Physical Geography*, *82*(2-3), 213–235.

Stenni, B., Buiron, D., Frezzotti, M., Albani, S., Barbante, C., Bard, E., ... Udisti, R. (2011, dec). Expression of the bipolar see-saw in Antarctic climate records during the last deglaciation. *Nature Geoscience*, *4*(1), 46–49. Retrieved from http://www.nature.com/doifinder/10.1038/ngeo1026 doi: 10.1038/ngeo1026

Sutter, J., Eisen, O., Werner, M., Grosfeld, K., Kleiner, T., & Fischer, H. (2020). Limited retreat of the wilkes basin ice sheet during the last interglacial. *Geophysical Research Letters*, *47*(13), e2020GL088131.

Sutter, J., Gierz, P., Grosfeld, K., Thoma, M., & Lohmann, G. (2016). Ocean temperature thresholds for last interglacial west antarctic ice sheet collapse. *Geophysical Research Letters*, *43*(6), 2675–2682.

Tindall, J. C., Valdes, P. J., & Sime, L. C. (2009, feb). Stable water isotopes in HadCM3: Isotopic signature of El Niño - Southern Oscillation and the tropical amount effect. *Journal of Geophysical Research*, *114*, 12pp. Retrieved from http://www.agu.org/pubs/crossref/2009/2008JD010825.shtml doi: 10.1029/2008JD010825

Werner, M., Jouzel, J., Masson-Delmotte, V., & Lohmann, G. (2018). Reconciling glacial antarctic water stable isotopes with ice sheet topography and the isotopic paleothermometer. *Nature Communications*, *9*(3537).

Wilson, D. J., Bertram, R. A., Needham, E. F., van de Flierdt, T., Welsh, K. J., McKay, R. M., ... Escutia, C. (2018). Ice loss from the east antarctic ice sheet

during late pleistocene interglacials. *Nature*, *561*(561), 383–386. Retrieved from https://doi.org/10.1038/s41586-018-0501-8

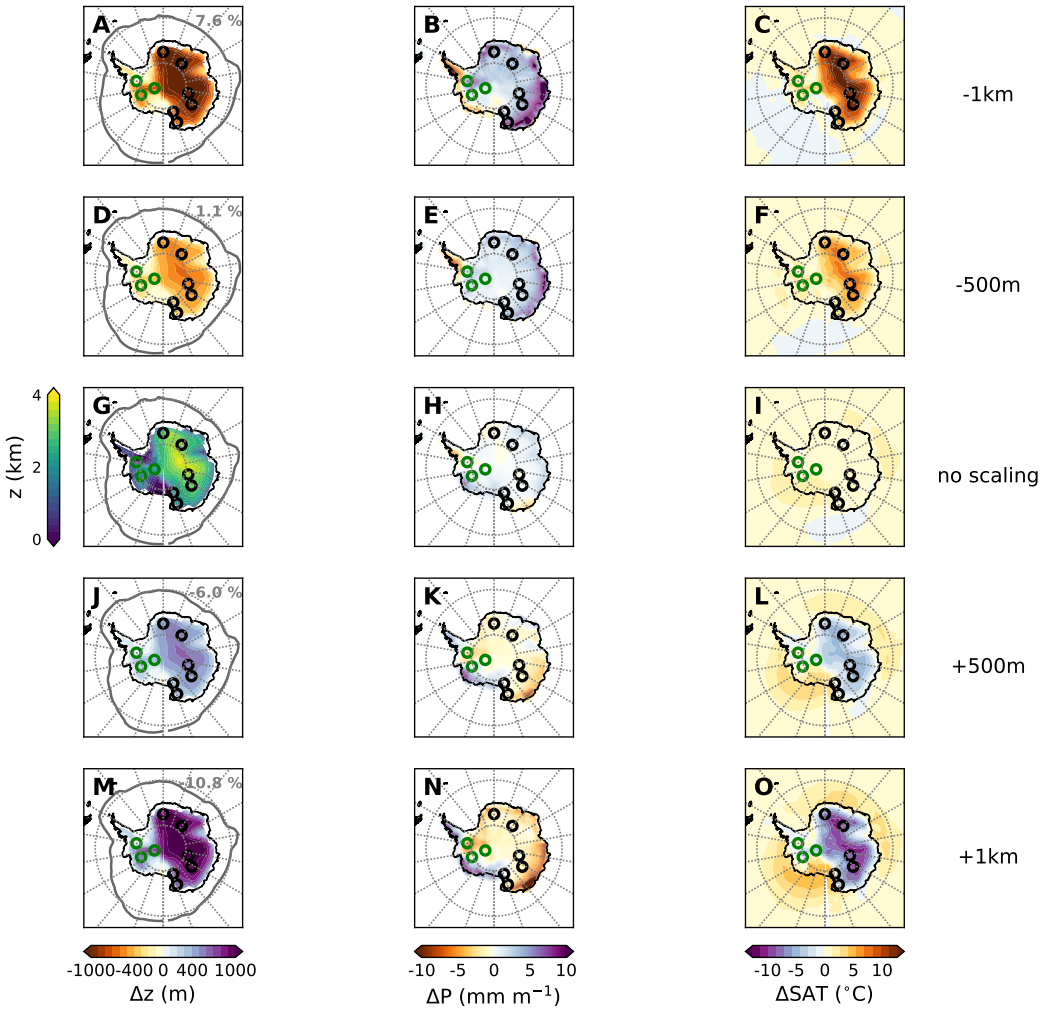

Figure 1. Patterns of idealised Antarctic Ice Sheet simulations. Map of Antarctic elevation change in response to elevation scaling of -1 km (first row); -500 m (second row); no scaling (third row); + 500 m (fourth); and +1 km (last row), relative to the height at EDC. Panel G represents the orography of the reference Antarctic configuration ("Z", in km). The different panels (with the exception of panel G) display anomalies relative to a pre-industrial control experiment using the reference Antarctic configuration, of (i) the orography ("ΔZ", in m, first column) with the September sea-ice extent (≥15%, grey contours), (ii) precipitation ("ΔP", in mm/month, second column), and (iii) the surface air temperature ("ΔSAT", in °C, third column). September sea-ice anomalies are given in the top right of the figures giving the orography and the September sea-ice extent. Ice core locations with available data are indicated by black points whereas ice core locations with no available data are indicated by green points.

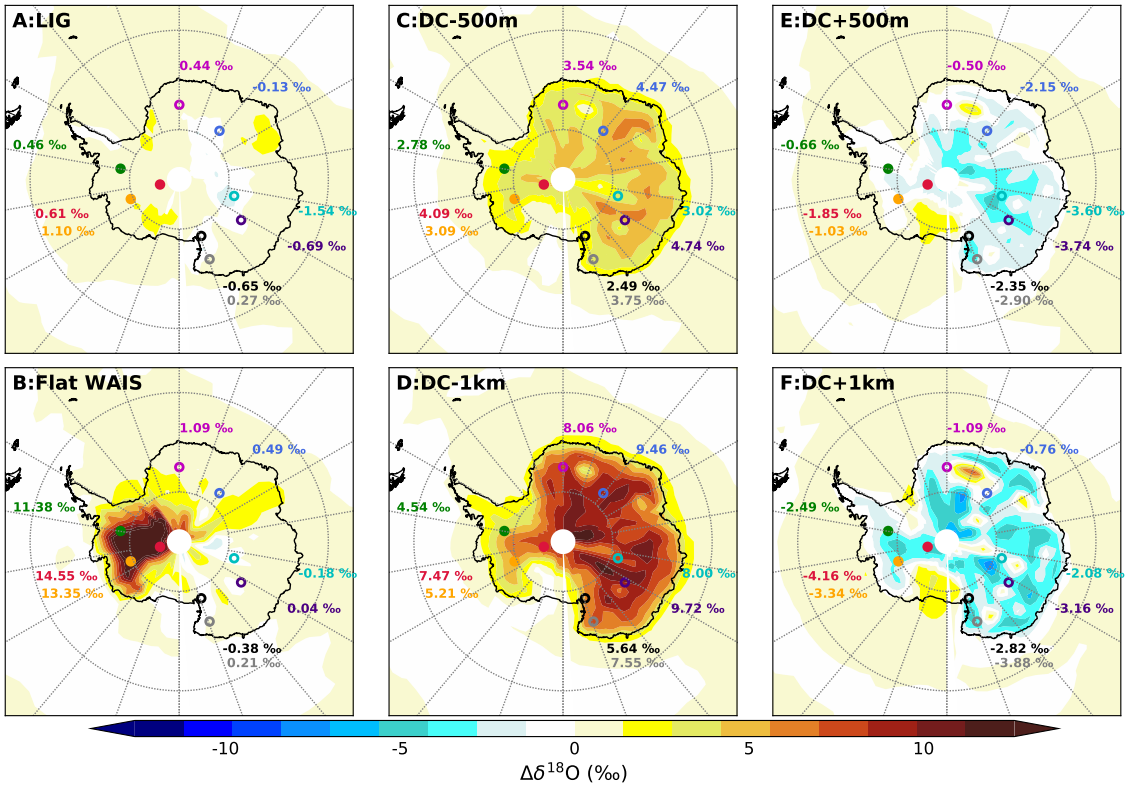

Figure 2. Patterns of $\Delta\delta^{18}$O anomalies. Maps of $\Delta\delta^{18}$O anomalies against the pre-industrial control experiment for (A) the Last Interglacial control experiment, (B) the "flat wais" experiment of Holloway et al. (2016) corresponding to a remanant 200 m West Antarctic Ice Sheet, our Antarctic elevation change in response to elevation scaling of (C) -500 m, (D) -1 km, (E) +500 m, and (F) +1 km, relative to the height at EDC. Points correspond to ice core locations: Vostok (dark green), Dome F (dark blue), EPICA Dome C (grey), EPICA Dronning Maud Land (red), Talos Dome (light green), Taylor Dome (dark violet), Hercules Dome (black), Skytrain (magenta). Filled points correspond to locations with no available δ^{18}O data.

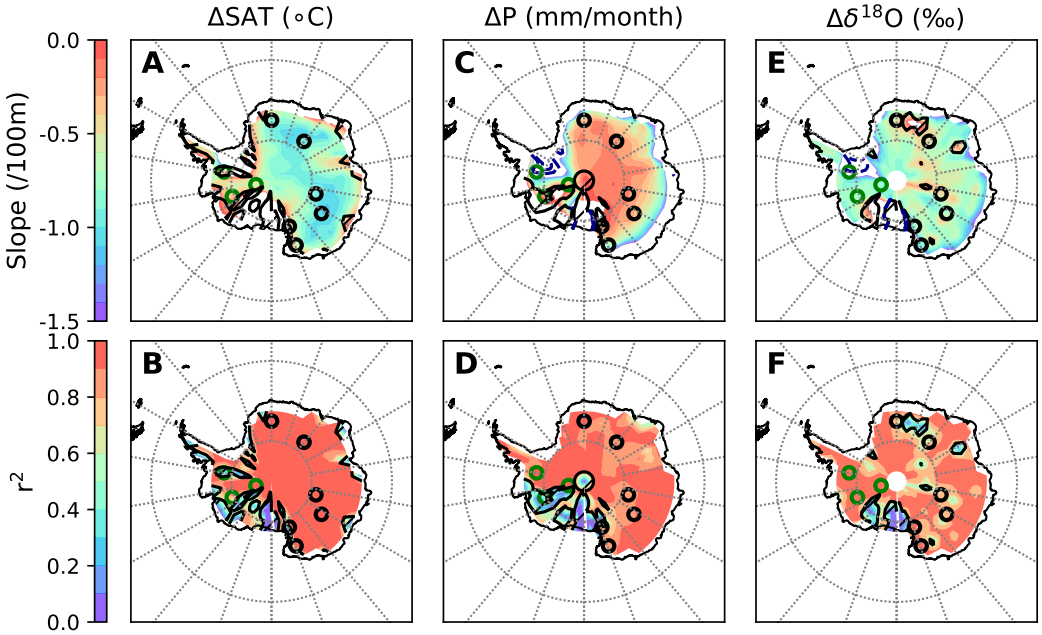

Figure 3. Continental-scale elevation gradients. Slopes ("Slope", panels A, C and E) and variance ("r^2", panels B, D and F) between the deviations of simulated surface air temperature ("ΔSAT", slope in °C/100m), precipitation ("ΔP", slope in mm/month/100m) and δ^{18}O ("$\Delta\delta^{18}$O", slope in ‰/100m) compared to the Last Interglacial control simulation, and the elevation at each grid point. In the Weddell region, slopes for precipitation and δ^{18}O can be particular low, and are thus shown by blue contours (-20 and -50 ° C/100m for temperature, -20 and -50 mm/month/100m). Non significant relationships are hatched. Ice core locations with available data are indicated by black points whereas locations with no available data are indicated by green points.

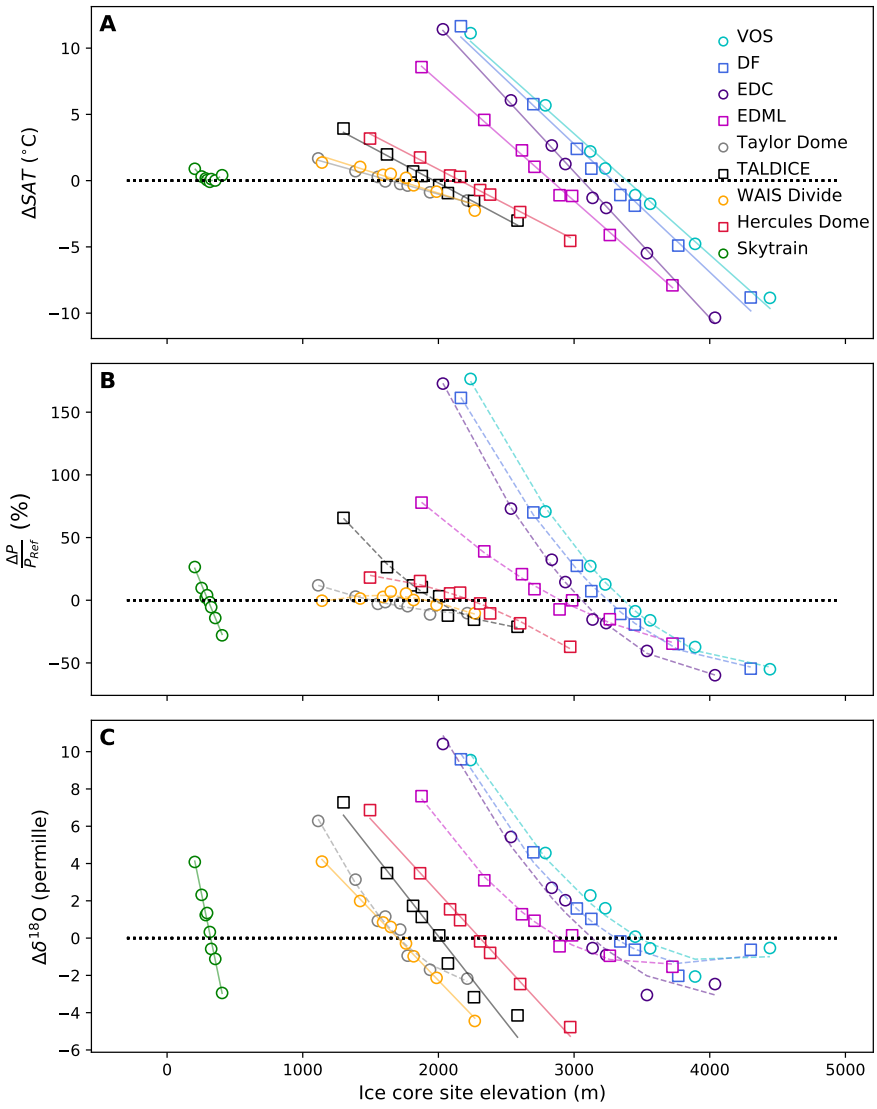

Figure 4. Ice core site elevation gradients. Deviations in ice core (A) surface air temperature ("ΔSAT", in °C), (B) precipitation flux ("$\Delta P/P_{Ref}$", in %), and (C) $\delta^{18}O$ ($\Delta\delta^{18}O$, in ‰) compared to the Last Interglacial control simulation, against the site elevation (in m) for a range of Antarctic ice core sites discussed in the text: Vostok ("VOS"), Dome F ("DF"), EPICA Dome C ("EDC"), EPICA Dronning Maud Land ("EDML"), Taylor Dome ("Taylor Dome"), Talos Dome ("TALDICE"), WAIS Divide ("WAIS Divide"), Hercules Dome ("Hercules Dome") and Skytrain ("Skytrain"). Dots are associated with ice core sites, solid lines emphasize strong linear relationships and dashed lines strong 2-degree polynomials (i.e. for correlation coefficients higher than 0.9).

Figure1.

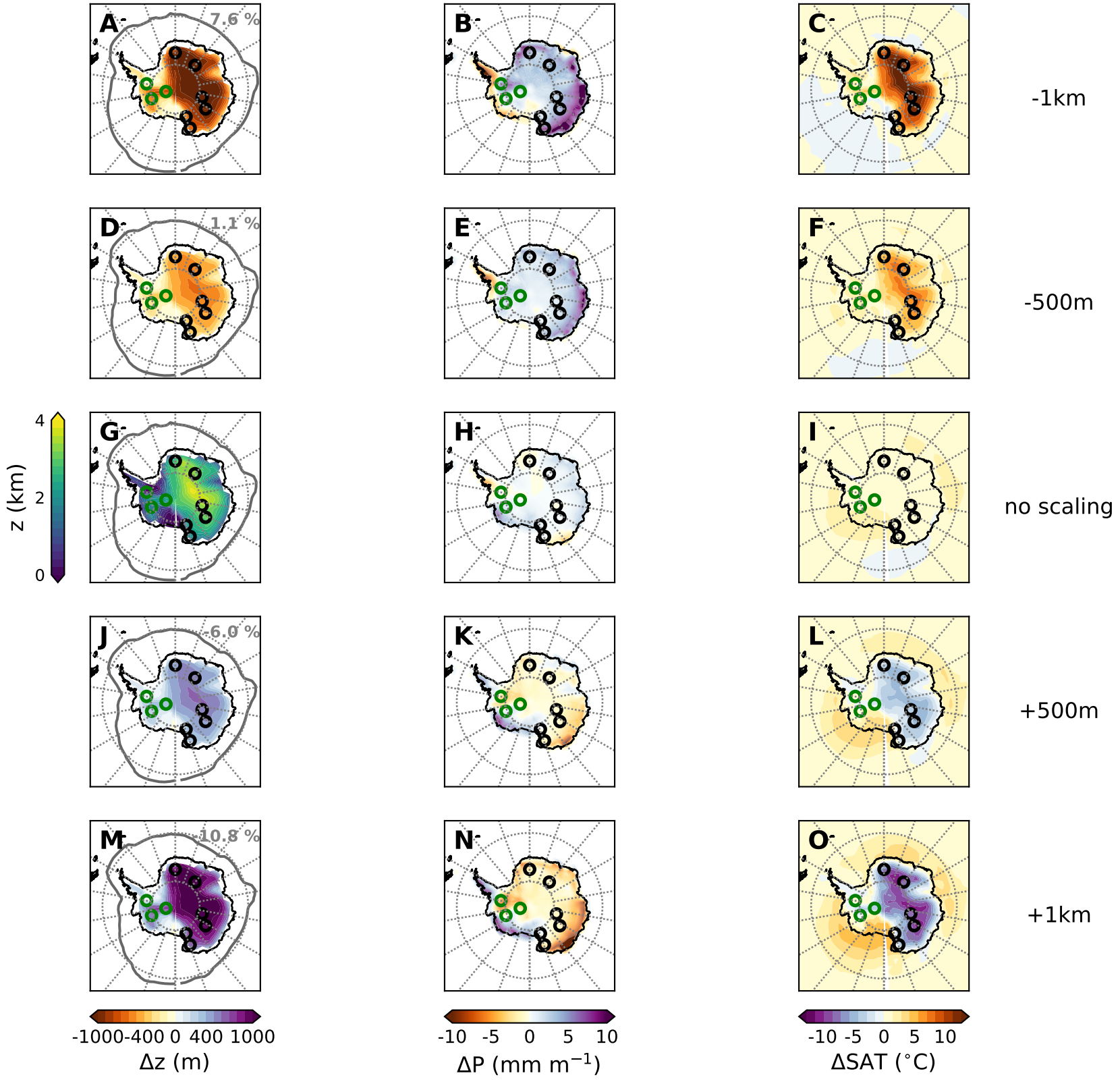
A
7.6 %
B
C
-1km
D
1.1 %
E
F
-500m
z (km)
4
2
0
G
H
I
no scaling
J
-6.0 %
K
L
+500m
M
-10.8 %
N
O
+1km
-1000 -400 0 400 1000
Δz (m)
-10 -5 0 5 10
ΔP (mm m^{-1})
-10 -5 0 5 10
ΔSAT (°C)

Figure2.

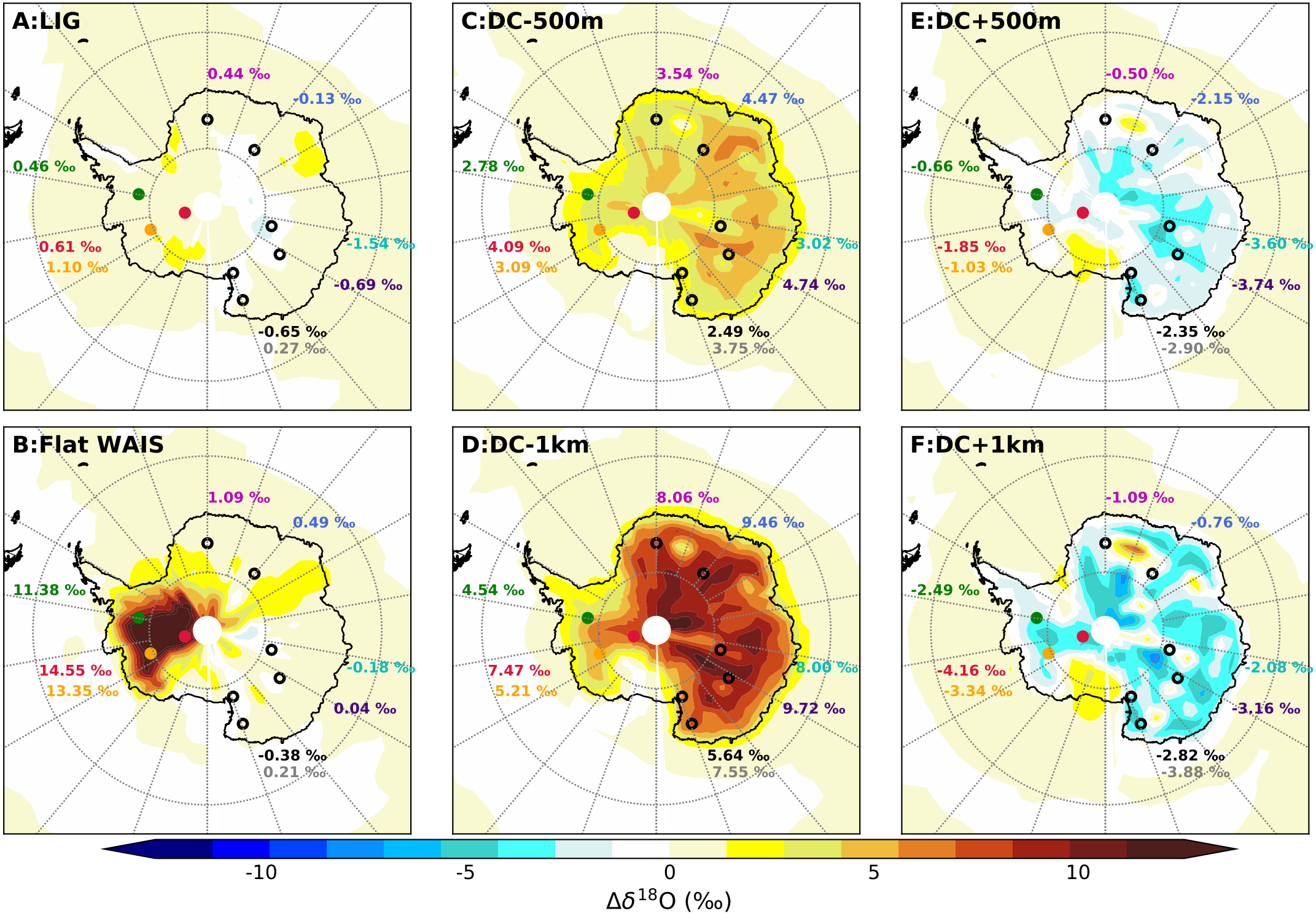
A:LIG
0.44 ‰
-0.13 ‰
0.46 ‰
0.61 ‰
1.10 ‰
-1.54 ‰
-0.69 ‰
-0.65 ‰
0.27 ‰
C:DC-500m
3.54 ‰
4.47 ‰
2.78 ‰
4.09 ‰
3.09 ‰
3.02 ‰
4.74 ‰
2.49 ‰
3.75 ‰
E:DC+500m
-0.50 ‰
-2.15 ‰
-0.66 ‰
-1.85 ‰
-1.03 ‰
-3.60 ‰
-3.74 ‰
-2.35 ‰
-2.90 ‰
B:Flat WAIS
1.09 ‰
0.49 ‰
11.38 ‰
14.55 ‰
13.35 ‰
-0.18 ‰
0.04 ‰
-0.38 ‰
0.21 ‰
D:DC-1km
8.06 ‰
9.46 ‰
4.54 ‰
7.47 ‰
5.21 ‰
8.00 ‰
9.72 ‰
5.64 ‰
7.55 ‰
F:DC+1km
-1.09 ‰
-0.76 ‰
-2.49 ‰
-4.16 ‰
-3.34 ‰
-2.08 ‰
-3.16 ‰
-2.82 ‰
-3.88 ‰
-10
-5
0
5
10
Δδ18O (‰)

Figure3.

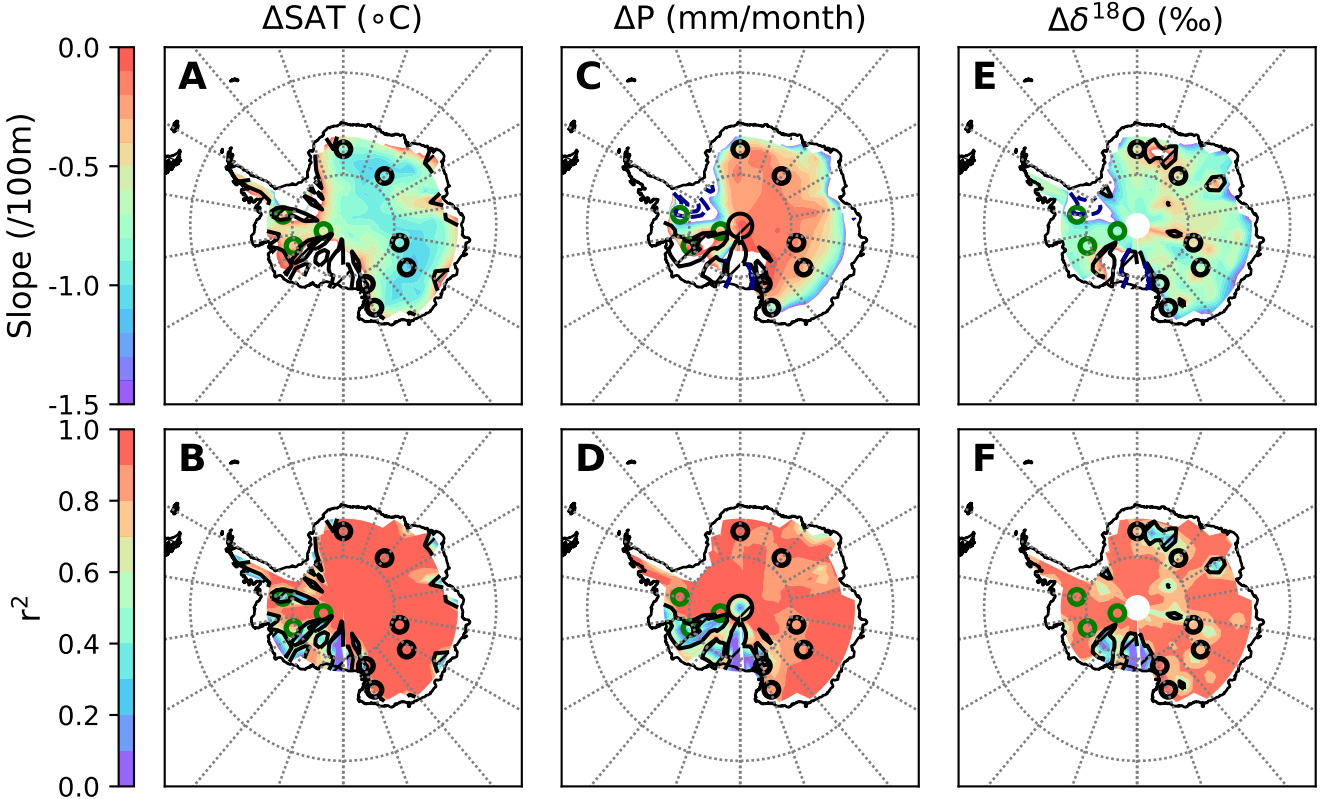
ΔSAT (∘C)
ΔP (mm/month)
Δδ18O (‰)
A
B
C
D
E
F
Slope (/100m)
0.0
-0.5
-1.0
-1.5
r2
1.0
0.8
0.6
0.4
0.2
0.0

Figure4.

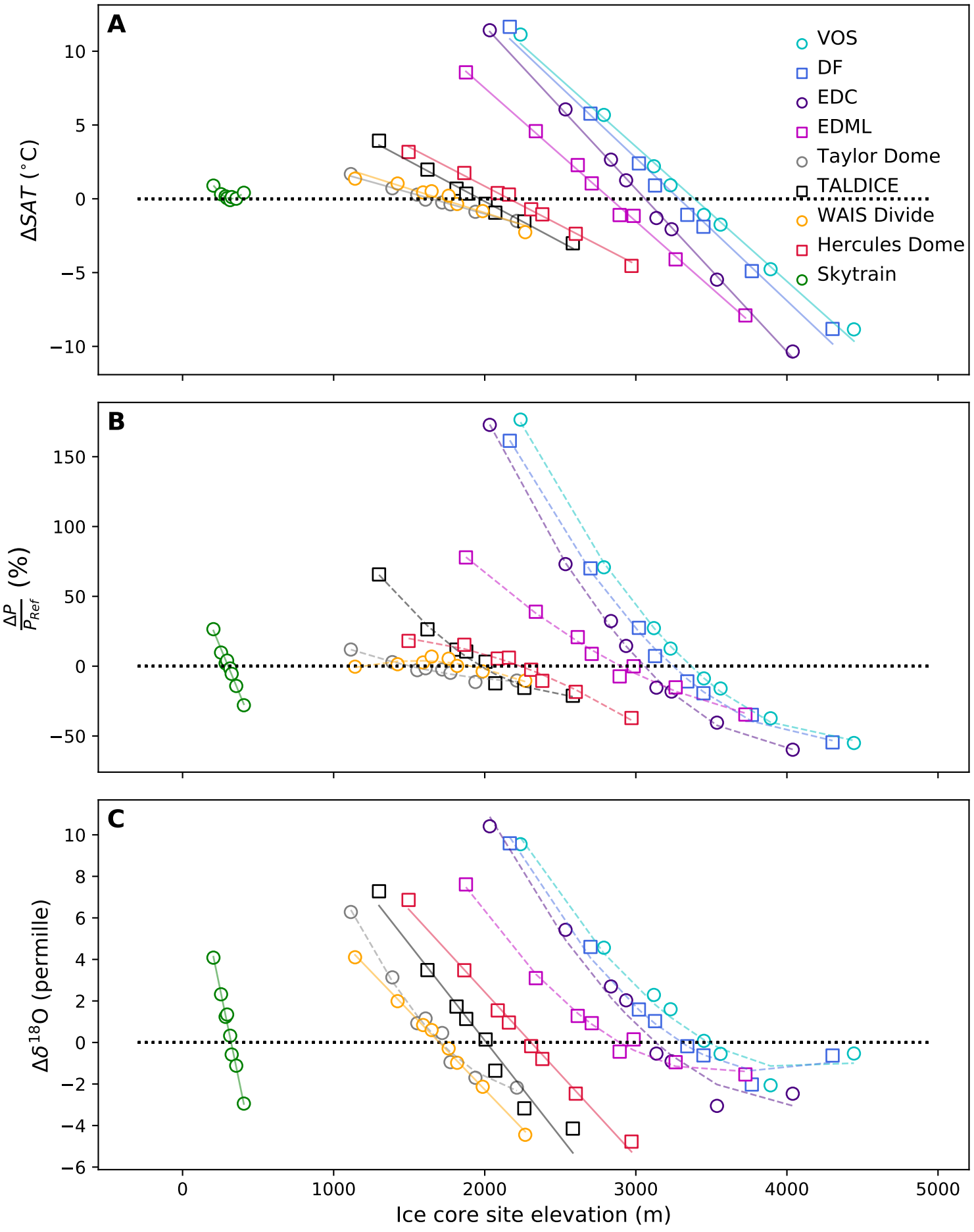
A
B
C
VOS
DF
EDC
EDML
Taylor Dome
TALDICE
WAIS Divide
Hercules Dome
Skytrain
ΔSAT (°C)
ΔP/P_Ref (%)
Δδ18O (permille)
Ice core site elevation (m)